

Efficient one-pot synthesis of pyrido[2,3-*d*]pyrimidines catalyzed by nanocrystalline MgO in water

Amaneh Mossafaii Rad¹ · Masoud Mokhtary¹

Received: 10 November 2014 / Accepted: 26 March 2015 / Published online: 15 April 2015
© The Author(s) 2015. This article is published with open access at Springerlink.com

Abstract The direct three-component condensation of 6-aminouracil, 6-amino-2-thiouracil or 6-amino-1,3-dimethyluracil, with arylaldehydes and malononitrile to generate a series of pyrido[2,3-*d*]pyrimidine derivatives has been carried out over nanocrystalline MgO with high efficiency in water as a green solvent at 80 °C. The morphology and structure of the nanocrystalline MgO were characterized by scanning electron microscopy, transmission electron microscopy and X-ray diffraction. The results confirmed the nanocrystalline MgO particle size is approximately 50 nm. This methodology offers significant improvements for the synthesis of pyrido[2,3-*d*]pyrimidine derivatives with regard to the yield of products, simplicity in operation, and green aspects by avoiding toxic catalysts and solvents.

Keywords Aminouracils · Pyrido[2,3-*d*]pyrimidines · Nanocrystalline MgO · Multicomponent reaction

Background

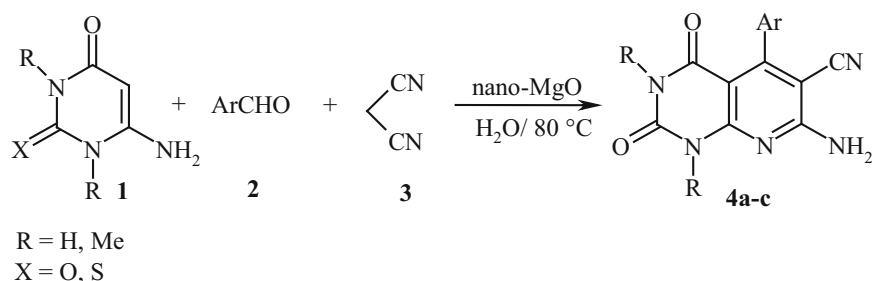
MgO is a particularly interesting material, since it has been the subject of extensive theoretical and experimental surface science studies. It exhibits optical properties and architectures and can be synthesized in a variety of

presentation formats, including nanosheets and nanoparticles [1]. Nano-MgO particles are attractive catalysts because of the large surface area they present. Nanocatalysts are considered to be a bridge between homogeneous and heterogeneous catalyst [2, 3]. Pyrido[2,3-*d*]pyrimidines are annulated uracil which have received considerable attention over the past years due to their wide range of biological and pharmacological activities such as antitumor [4], antihypertensive and hepatoprotective [5], cardiogenic [6] and antifolate [7]. Uracil derivatives are versatile building blocks for the synthesis of nitrogen-containing heteroaromatic species of biological importance [8]. Pyrazolopyridines [9], pyrimidopyrimidines [10], pyridopurines [11], pyrazolopyrimidines [12] and xanthine derivatives [13] have all been prepared by the functionalization of uracil derivatives. The diverse range of biological activities of uracil derivatives in parasitic chemotherapy has stimulated considerable interest in their synthesis. Therefore, a number of reports have appeared in the literatures such as palladium-catalyzed oxidative coupling [14], nucleophilic-induced ring transformation [15], KF–Al₂O₃ [16], *L*-proline [17], triethylbenzylammonium chloride (TEBAC) [18], diammonium hydrogen phosphate (DAHP) [19] and tetra-*n*-butyl ammonium bromide (TBAB) [20]. Most of these reported methods require a forcing conditions, high temperature, long reaction times and complex synthetic pathways. Thus new routes for the synthesis of these molecules have attracted considerable attention in search for a rapid entry to these heterocycles. Herein, nanocrystalline MgO has been successfully applied to perform the reaction of 6-aminouracil, 6-amino-2-thiouracil or 6-amino-1,3-dimethyluracil with malononitrile and aldehydes in water at 80 °C to provide a series of pyrido[2,3-*d*]pyrimidine derivatives in high yields (Scheme 1).

✉ Masoud Mokhtary
mmokhtary@iaurasht.ac.ir

¹ Department of Chemistry, Rasht Branch, Islamic Azad University, Rasht, Iran

Scheme 1 Pyrido[2,3-*d*]pyrimidine derivatives by nanocrystalline MgO



Methods

The nanocrystalline MgO was purchased from Tecnan Spanish Company. The crystalline structure of the powders was investigated by X-ray diffraction (INEL Equinox) with Cu-K α , radiation, $\lambda = 0.1541874 \text{ \AA}$ radiation. The surface area of nanocrystalline MgO was observed using N₂ adsorption-desorption isotherms with surface analyzer equipment at 77 K. The size and morphology of the nanocrystalline MgO were determined using a transmission electron microscope (TEM, Philips EM208) and a scanning electron microscope (SEM, Philips $\times 130$). The NMR spectra were recorded in DMSO-*d*₆ with TMS as an internal standard on a Bruker Avance DRX 400 MHz spectrometer. FT-IR spectra were determined on an SP-1100, P-UV-Com instrument. The products were characterized by FT-IR, ¹H NMR, ¹³C NMR and by comparison with authentic samples reported in the literature.

General synthesis of pyrido[2,3-*d*]pyrimidines

A mixture of aromatic aldehyde (1 mmol), 6-aminouracil, 6-amino-2-thiouracil or 6-amino-1,3-dimethyluracil (1 mmol) and malononitrile (1 mmol) in the presence of nanocrystalline MgO (0.25 mmol) was stirred in water (5 ml) at 80 °C for the appropriate time, as shown in Table 1. Completion of the reaction was indicated by TLC monitoring. The nanocrystalline MgO was filtered off and the reaction mixture was cooled to ambient temperature, and the crude solid residue was recrystallized from ethanol and water to afford pure crystals of the proper pyrido[2,3-*d*]pyrimidines in 84–96 % yields.

Spectral data of new products are provided below

7-Amino-1,3-dimethyl-5-(3-nitrophenyl)-2,4-dioxo-1,2,3,4-tetrahydropyrido[2,3-*d*] pyrimidine-6-carbonitrile (4f)

Mp >300 °C. FT-IR (KBr): 3456, 3313 (NH₂ stretch), 3224 (aromatic C–H stretch), 2206 (C \equiv N stretch), 1664, 1625 (C=O stretch), 1566, 1510 (aromatic C=C stretch), 1440 (NO₂

Table 1 Synthesis of pyrido[2,3-*d*]pyrimidine derivatives by nanocrystalline MgO

Entry	X	R	Aryl	Product	Time (min)	Yield (%) ^a
1	O	H	C ₆ H ₅	4a	18	92
2	O	H	2-Cl-C ₆ H ₄	4b	15	89
3	O	H	4-Cl-C ₆ H ₄	4c	12	96
4	O	H	4-MeO-C ₆ H ₄	4d	30	88
5	O	H	4-Me-C ₆ H ₄	4e	35	87
6	O	Me	3-NO ₂ -C ₆ H ₄	4f	30	90
7	O	Me	4-NO ₂ -C ₆ H ₄	4g	20	95
8	O	Me	4-Cl-C ₆ H ₄	4h	15	90
9	O	Me	3-Cl-C ₆ H ₄	4i	20	86
10	O	Me	2-Cl-C ₆ H ₄	4j	25	84
11	O	Me	3-Br-C ₆ H ₄	4k	15	86
12	O	Me	4-F-C ₆ H ₄	4l	25	90
13	S	H	C ₆ H ₅	4m	20	88
14	S	H	4-Cl-C ₆ H ₄	4n	16	90
15	S	H	4-Br-C ₆ H ₄	4o	15	90
16	S	H	4-F-C ₆ H ₄	4p	12	92

Reaction and conditions: 6-aminouracil, 6-amino-2-thiouracil or 6-amino-1,3-dimethyluracil (1 mmol), aldehyde (1 mmol), malononitrile (1 mmol) and nanocrystalline MgO (0.25 mmol) in H₂O (5 mL) at 80 °C

^a All yields refer to isolated products

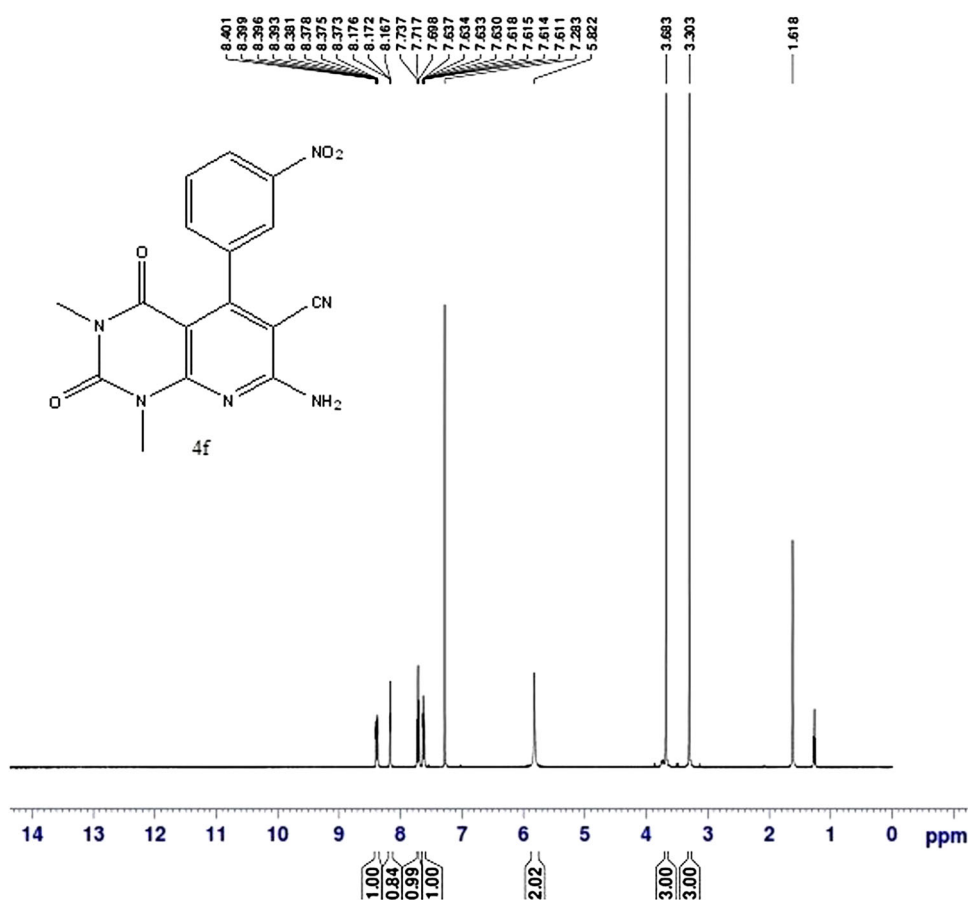
asymmetric stretch), 1363 (NO₂ symmetric stretch), 1278, 1217 (symmetric C–H bend, CH₃), 838, 806, 750 (aromatic C–H out of plane bending) cm⁻¹; ¹H NMR (400 MHz, CDCl₃): δ ; 3.30 (s, 3H, CH₃), 3.68 (s, 3H, CH₃), 5.82 (s, 2H, NH₂), 7.62 (m, 1H), 7.71 (t, $J = 7.8 \text{ Hz}$, 1H), 8.17 (t, $J = 8.1 \text{ Hz}$, 1H), 8.39 (m, 1H) ppm (Fig. 1); ¹³C NMR (100 MHz, CDCl₃): δ ; 159.9 (C=O amide), 159.0, 157.1, 154.1, 151.0, 148.0, 137.7, 133.1, 129.5, 124.0, 122.7, 114.6 (C \equiv N), 100.2, 89.7, 30.3 (CH₃), 28.4 (CH₃) ppm (Fig. 2).

7-Amino-1,3-dimethyl-5-(4-nitrophenyl)-2,4-dioxo-1,2,3,4-tetrahydropyrido[2,3-*d*] pyrimidine-6-carbonitrile (4g)

Mp >300 °C. FT-IR (KBr): 3442, 3311 (NH₂ stretch), 3217 (aromatic C–H stretch), 2212 (C \equiv N stretch), 1712, 1635 (C=O stretch), 1558, 1506 (aromatic C=C stretch),



Fig. 1 ^1H NMR spectra of 7-amino-1,3-dimethyl-5-(3-nitrophenyl)-2,4-dioxo-1,2,3,4-tetrahydropyrido[2,3-d]pyrimidine-6-carbonitrile



1444 (NO_2 asymmetric stretch), 1375 (NO_2 symmetric stretch), 1272, 1224 (symmetric C–H bend, CH_3), 968, 848 (aromatic C–H out of plane bending) cm^{-1} ; ^1H NMR (400 MHz, DMSO-d_6): δ : 3.08 (s, 3H, CH_3), 3.51 (s, 3H, CH_3), 7.50 (dd, $J = 6.9, 1.9$ Hz, 2H), 8.00 (s, 2H, NH_2), 8.31 (dd, $J = 6.9, 1.9$ Hz, 2H) ppm (Fig. 3); ^{13}C NMR (100 MHz, DMSO-d_6): δ : 160.1, 158.6, 157.0 ($\text{C}=\text{O}$ amide), 153.5, 150.8, 147.3, 144.4, 128.9, 123.0, 114.9 ($\text{C}\equiv\text{N}$), 98.3, 87.8, 29.6 (CH_3), 27.7 (CH_3) ppm (Fig. 4).

7-Amino-5-(4-chlorophenyl)-1,3-dimethyl-2,4-dioxo-1,2,3,4-tetrahydropyrido[2,3-d] pyrimidine-6-carbonitrile (4h)

$\text{Mp} > 300$ °C. FT-IR (KBr): 3568, 3458 (NH_2 stretch), 3216 (aromatic C–H stretch), 2214 ($\text{C}\equiv\text{N}$ stretch), 1714, 1714, 1654 ($\text{C}=\text{O}$ stretch), 1622, 1566, 1515 (aromatic C=C stretch), 1274, 1230 (symmetric C–H bend, CH_3), 750 ($\text{C}-\text{Cl}$ stretch), 700, 659 (aromatic C–H out of plane bending) cm^{-1} ; ^1H NMR (400 MHz, DMSO-d_6): δ : 3.09 (s, 3H, CH_3), 3.51 (s, 3H, CH_3), 7.28 (dd, $J = 6.6, 1.8$ Hz, 2H), 7.51 (dd, $J = 6.6, 1.8$ Hz, 2H), 7.93 (s, 2H, NH_2) ppm (Fig. 5); ^{13}C NMR (100 MHz, DMSO-d_6): δ : 160.2 ($\text{C}=\text{O}$ amide), 160.1, 158.5, 158.0, 153.6 ($\text{C}=\text{O}$ amide), 150.8,

136.1, 132.96, 129.2, 127.9, 115.2 ($\text{C}\equiv\text{N}$), 98.6, 88.3, 29.6 (CH_3), 28.0 (CH_3) ppm (Fig. 6).

7-Amino-5-(3-chlorophenyl)-1,3-dimethyl-2,4-dioxo-1,2,3,4-tetrahydropyrido[2,3-d] pyrimidine-6-carbonitrile (4i)

$\text{Mp} > 300$ °C. FT-IR (KBr): 3461, 3334 (NH_2 stretch), 3228 (aromatic C–H stretch), 2219 ($\text{C}\equiv\text{N}$ stretch), 1712, 1672 ($\text{C}=\text{O}$ stretch), 1637, 1508 (aromatic C=C stretch), 1276, 1224 (symmetric C–H bend, CH_3), 975 ($\text{C}-\text{Cl}$ stretch), 790, 748, 705 (aromatic C–H out of plane bending) cm^{-1} ; ^1H NMR (400 MHz, DMSO-d_6): δ : 3.09 (s, 3H, CH_3), 3.51 (s, 3H, CH_3), 7.21 (d, $J = 6.8$ Hz, 1H, H_c), 7.34 (s, 1H), 7.48 (m, 2H), 7.93 (s, 2H, NH_2) ppm (Fig. 7); ^{13}C NMR (100 MHz, DMSO-d_6): δ : 160.2, 160.1, 158.4, 157.5 ($\text{C}=\text{O}$ amide), 153.5, 150.8, 139.3, 132.4, 129.8, 128.0, 127.0, 126.0, 115.1 ($\text{C}\equiv\text{N}$), 98.6, 88.3, 29.6 (CH_3), 27.7 (CH_3) ppm (Fig. 8).

7-Amino-5-(2-chlorophenyl)-1,3-dimethyl-2,4-dioxo-1,2,3,4-tetrahydropyrido[2,3-d] pyrimidine-6-carbonitrile (4j)

$\text{Mp} > 300$ °C. FT-IR (KBr): 3460, 3315 (NH_2 stretch), 3218 (aromatic C–H stretch), 2210 ($\text{C}\equiv\text{N}$ stretch), 1716,

Fig. 2 ^{13}C NMR spectra of 7-amino-1,3-dimethyl-5-(3-nitrophenyl)-2,4-dioxo-1,2,3,4-tetrahydropyrido[2,3-d]pyrimidine-6-carbonitrile

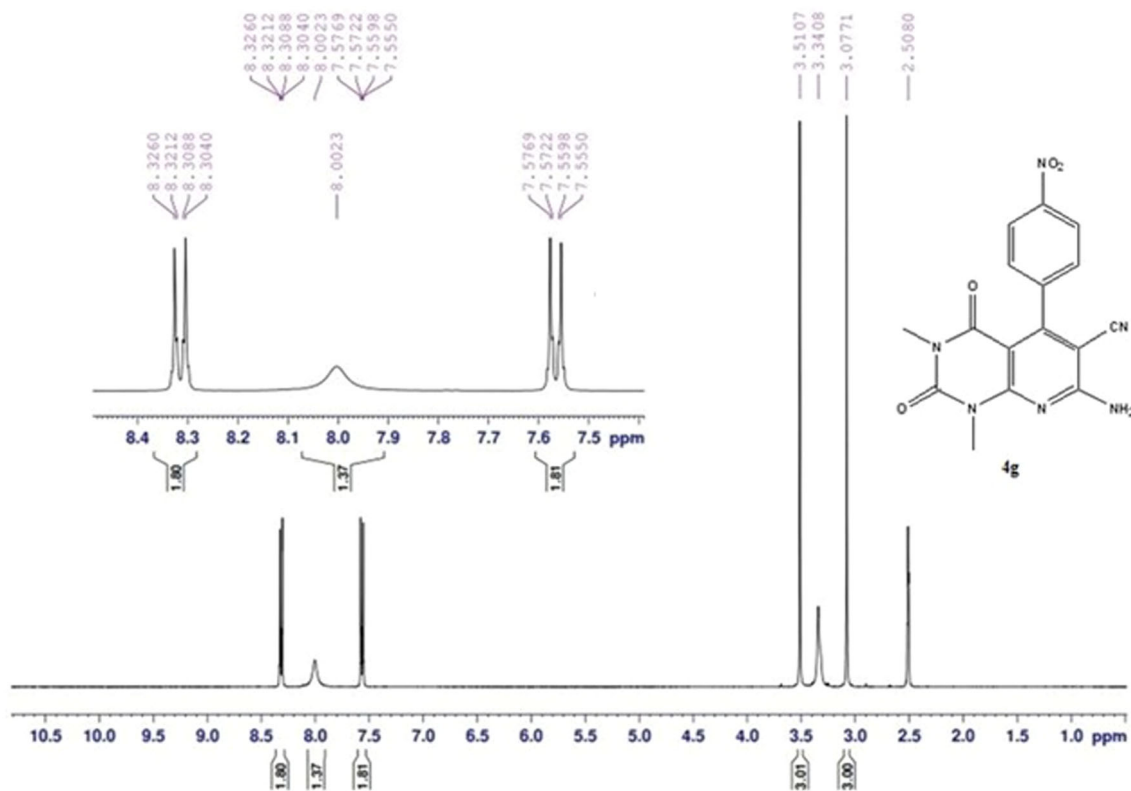
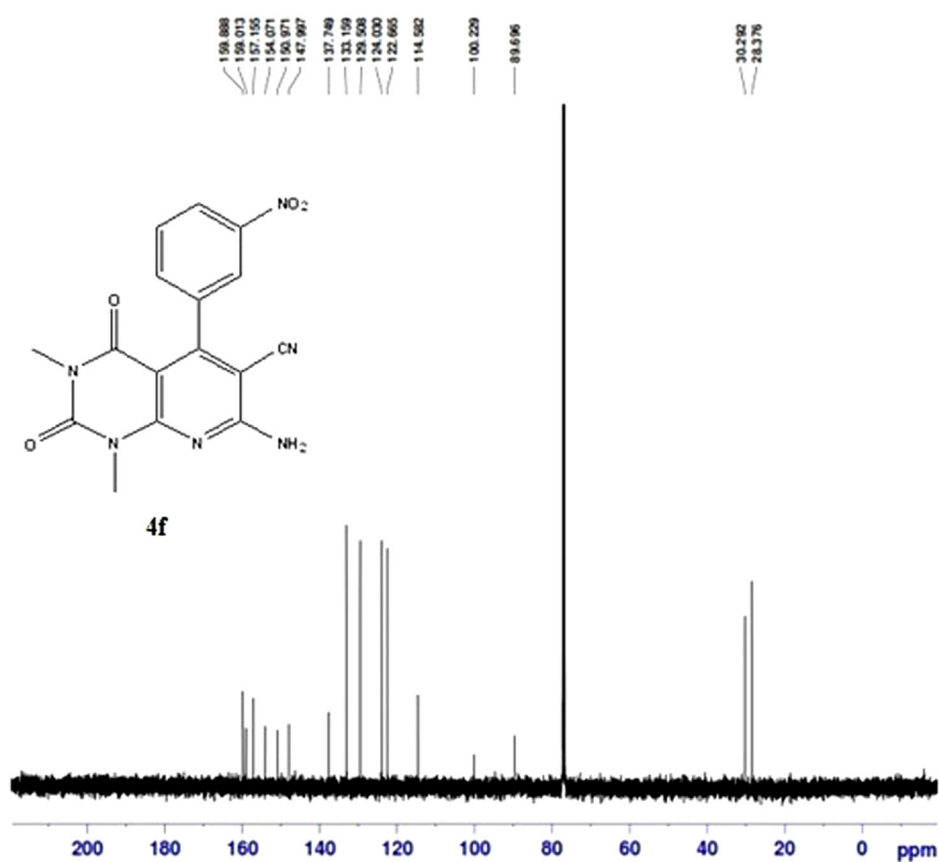


Fig. 3 ^1H NMR spectra of 7-amino-1,3-dimethyl-5-(4-nitrophenyl)-2,4-dioxo-1,2,3,4-tetrahydropyrido[2,3-d]pyrimidine-6-carbonitrile



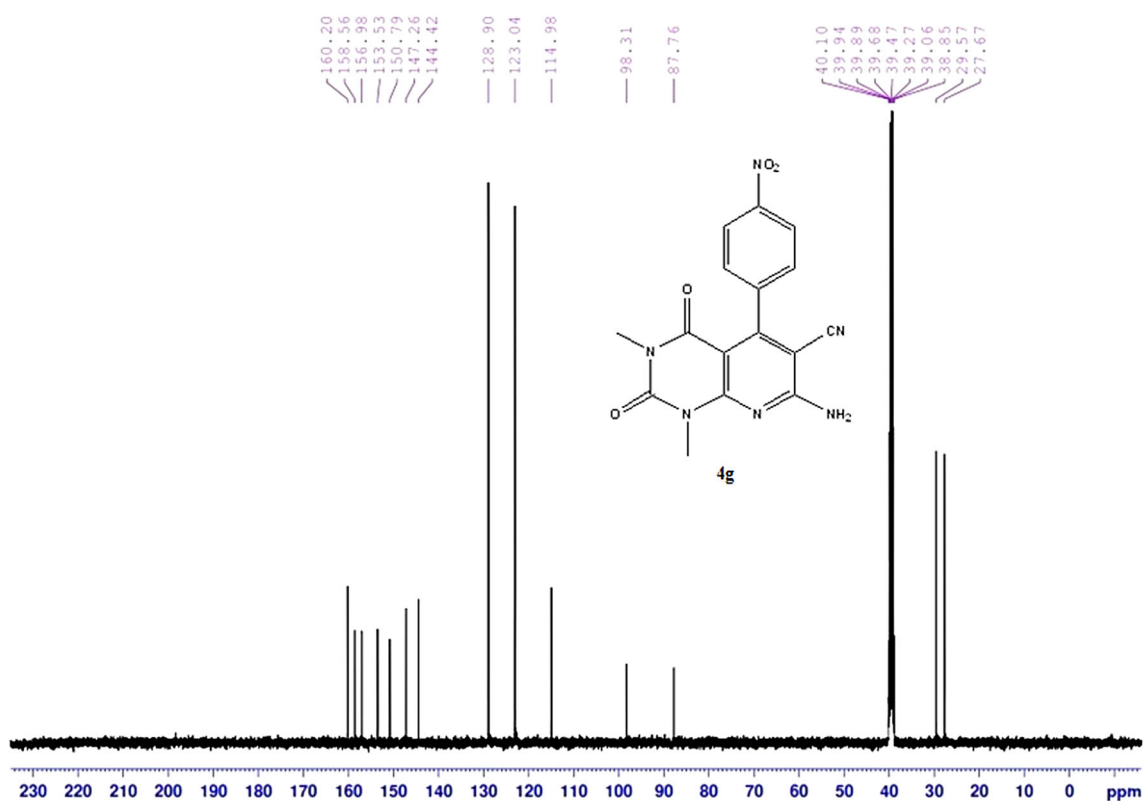


Fig. 4 ^{13}C NMR spectra of 7-amino-1,3-dimethyl-5-(4-nitrophenyl)-2,4-dioxo-1,2,3,4-tetrahydropyrido[2,3-d]pyrimidine-6-carbonitrile

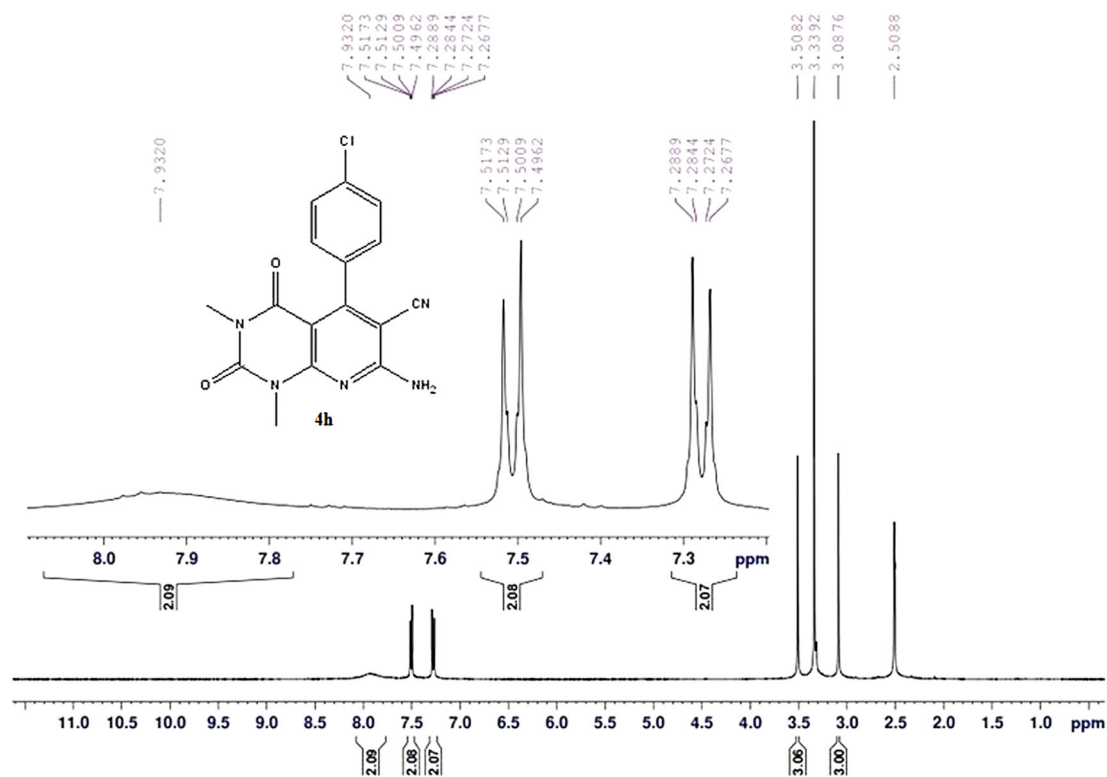


Fig. 5 ^1H NMR spectra of 7-amino-5-(4-chlorophenyl)-1,3-dimethyl-2,4-dioxo-1,2,3,4-tetrahydropyrido[2,3-d] pyrimidine-6-carbonitrile

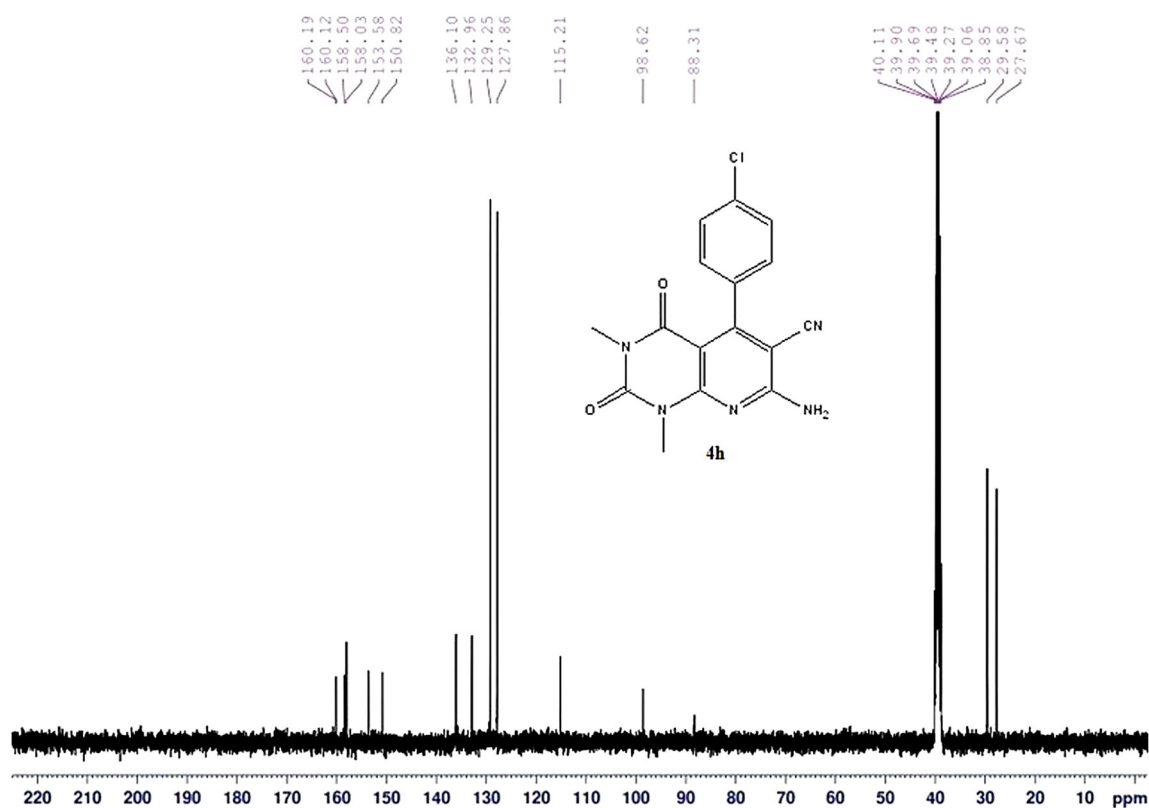


Fig. 6 ^{13}C NMR spectra of 7-amino-5-(4-chlorophenyl)-1,3-dimethyl-2,4-dioxo-1,2,3,4-tetrahydropyrido[2,3-d] pyrimidine-6-carbonitrile

1658 (C=O stretch), 1620, 1568 (aromatic C=C stretch), 1278, 1230 (symmetric C–H bend, CH_3), 748 (C–Cl stretch), 700, 659 (aromatic C–H out of plane bending) cm^{-1} ; ^1H NMR (400 MHz, DMSO-d_6): δ ; 3.10 (s, 3H, CH_3), 3.52 (s, 3H, CH_3), 7.26 (dd, $J = 7.8, 1.2$ Hz, 1H), 7.44 (m, 2H), 7.55 (dd, $J = 7.8, 1.2$ Hz, 1H), 7.99 (s, 2H, NH_2) ppm (Fig. 9); ^{13}C NMR (100 MHz, DMSO-d_6): δ ; 160.4, 160.3, 158.2, 156.2 (C=O amide), 153.5, 150.7, 136.3, 130.4, 129.9, 128.8, 128.7, 127.0, 114.7 (C \equiv N), 98.7, 88.1, 29.6 (CH_3), 27.6 (CH_3) ppm (Fig. 10).

7-Amino-5-(3-bromophenyl)-1,3-dimethyl-2,4-dioxo-1,2,3,4-tetrahydropyrido[2,3-d] pyrimidine-6-carbonitrile (4k)

Mp >300 °C. FT-IR (KBr): 3454, 3309 (NH_2 stretch), 3213 (aromatic C–H stretch), 2210 (C \equiv N stretch), 1712, 1662 (C=O stretch), 1623, 1554 (aromatic C=C stretch), 1434, 1365 (symmetric C–H bend, CH_3), 748 (C–Br stretch) cm^{-1} ; ^1H NMR (400 MHz, CDCl_3): δ ; 3.32 (s, 3H, CH_3), 3.70 (s, 3H, CH_3), 5.74 (s, 2H, NH_2), 7.38 (s, 1H), 7.40 (m, 2H), 7.64

(m, 1H) ppm (Fig. 11); ^{13}C NMR (100 MHz, CDCl_3): δ ; 159.8 (C=O amide), 158.9, 158.3, 154.0, 151.1, 148.1, 138.1, 134.9, 132.2, 130.0, 129.9, 125.6, 122.3, 114.8 (C \equiv N), 89.9, 30.2 (CH_3), 28.4 (CH_3) ppm (Fig. 12).

7-Amino-5-(4-fluorophenyl)-1,3-dimethyl-2,4-dioxo-1,2,3,4-tetrahydropyrido[2,3-d] pyrimidine-6-carbonitrile (4l)

Mp >300 °C. FT-IR (KBr): 3469, 3319 (NH_2 stretch), 3217 (aromatic C–H stretch), 2212 (C \equiv N stretch), 1708, 1649 (C=O stretch), 1622, 1554, 1508 (aromatic C=C stretch), 1276, 1226 (symmetric C–H bend, CH_3), 973 (C–F stretch), 850, 806, 752 (aromatic C–H out of plane bending) cm^{-1} ; ^1H NMR (400 MHz, DMSO-d_6): δ ; 3.09 (s, 3H, CH_3), 3.50 (s, 3H, CH_3), 7.25 (m, 2H), 7.30 (m, 2H), 7.89 (s, 2H, NH_2) ppm (Fig. 13); ^{13}C NMR (100 MHz, DMSO-d_6): δ ; 163.2 (C=S), 160.8 (C=O amide), 160.1, 159.4, 158.3, 153.6, 150.8, 133.3, 129.6, 115.3 (C \equiv N), 114.8, 114.6, 98.7, 88.6, 88.5, 29.6 (CH_3), 27.7 (CH_3) ppm (Fig. 14).

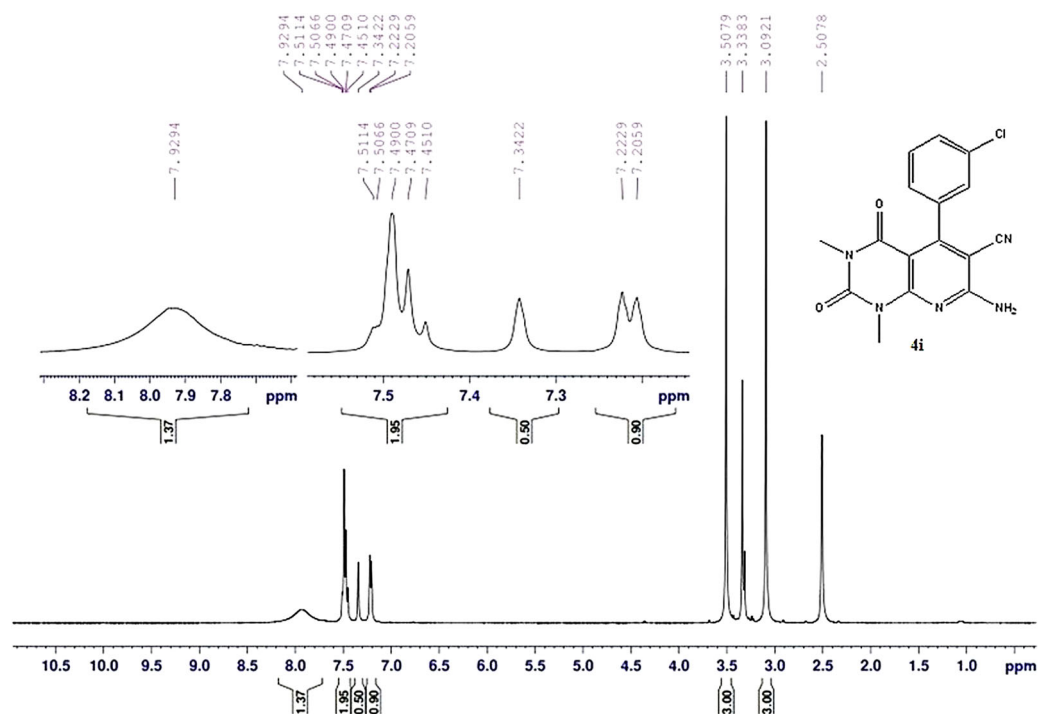


Fig. 7 ¹H NMR spectra of 7-amino-5-(3-chlorophenyl)-1,3-dimethyl-2,4-dioxo-1,2,3,4-tetrahydropyrido[2,3-d] pyrimidine-6-carbonitrile

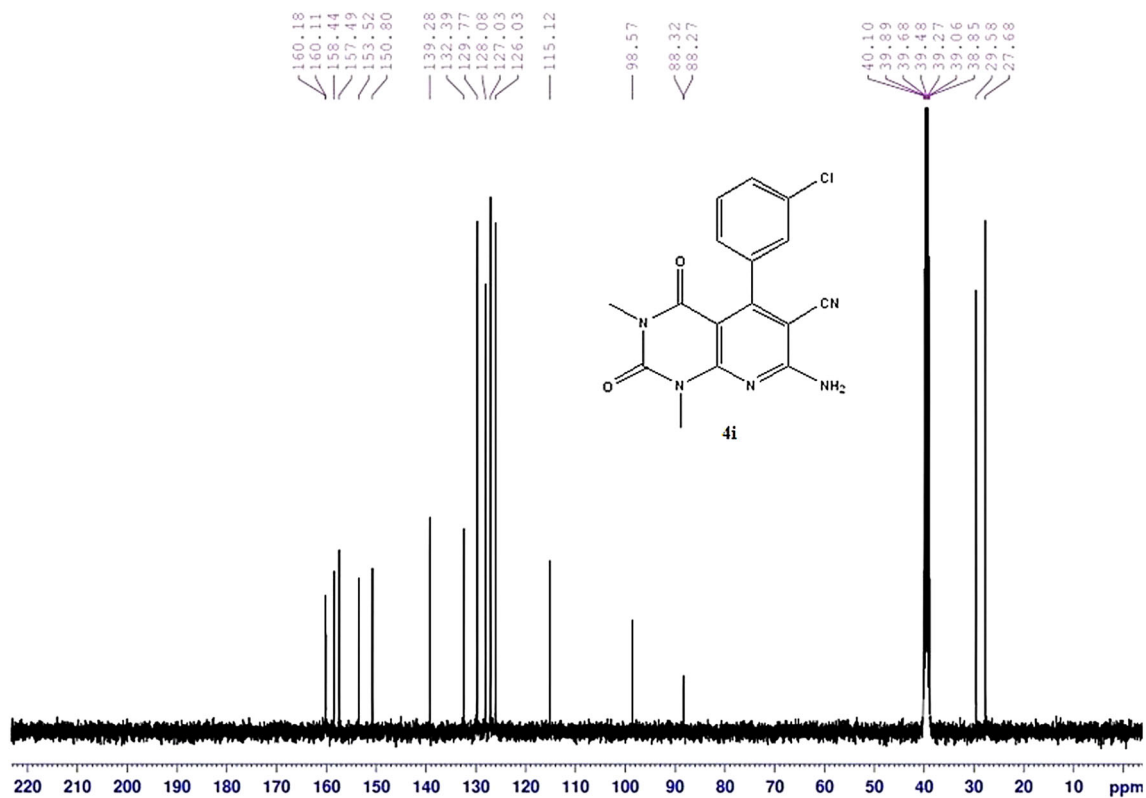


Fig. 8 ¹³C NMR spectra of 7-amino-5-(3-chlorophenyl)-1,3-dimethyl-2,4-dioxo-1,2,3,4-tetrahydropyrido[2,3-d] pyrimidine-6-carbonitrile

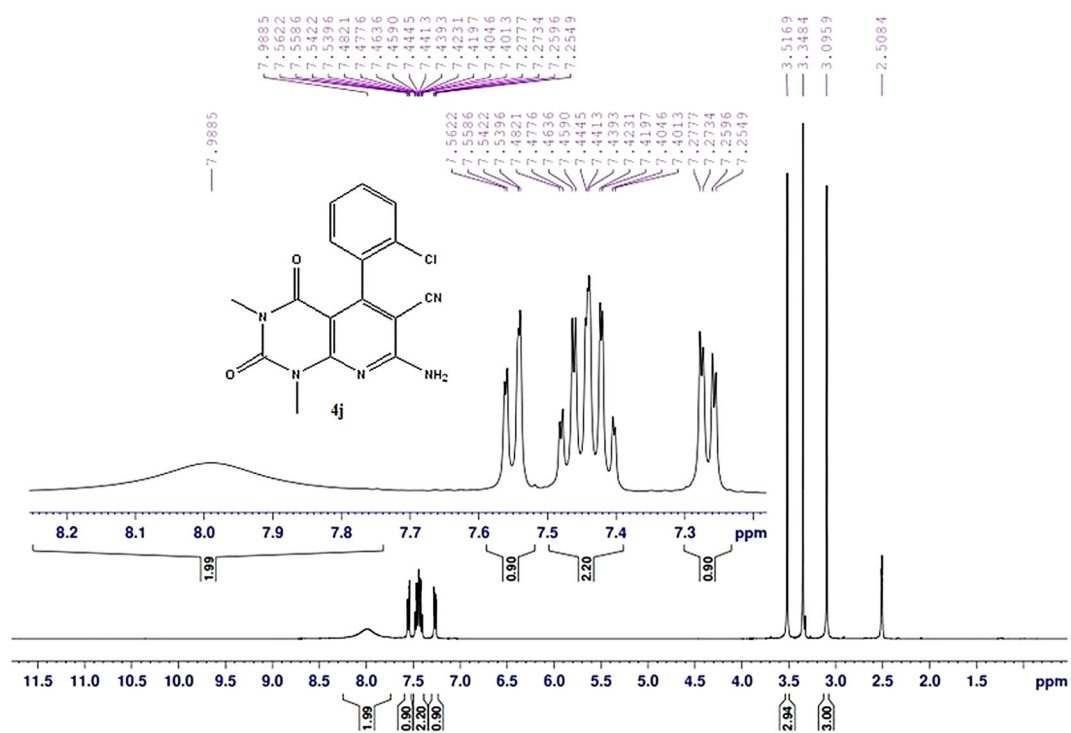


Fig. 9 ¹H NMR spectra of 7-amino-5-(2-chlorophenyl)-1,3-dimethyl-2,4-dioxo-1,2,3,4-tetrahydropyrido[2,3-d] pyrimidine-6-carbonitrile

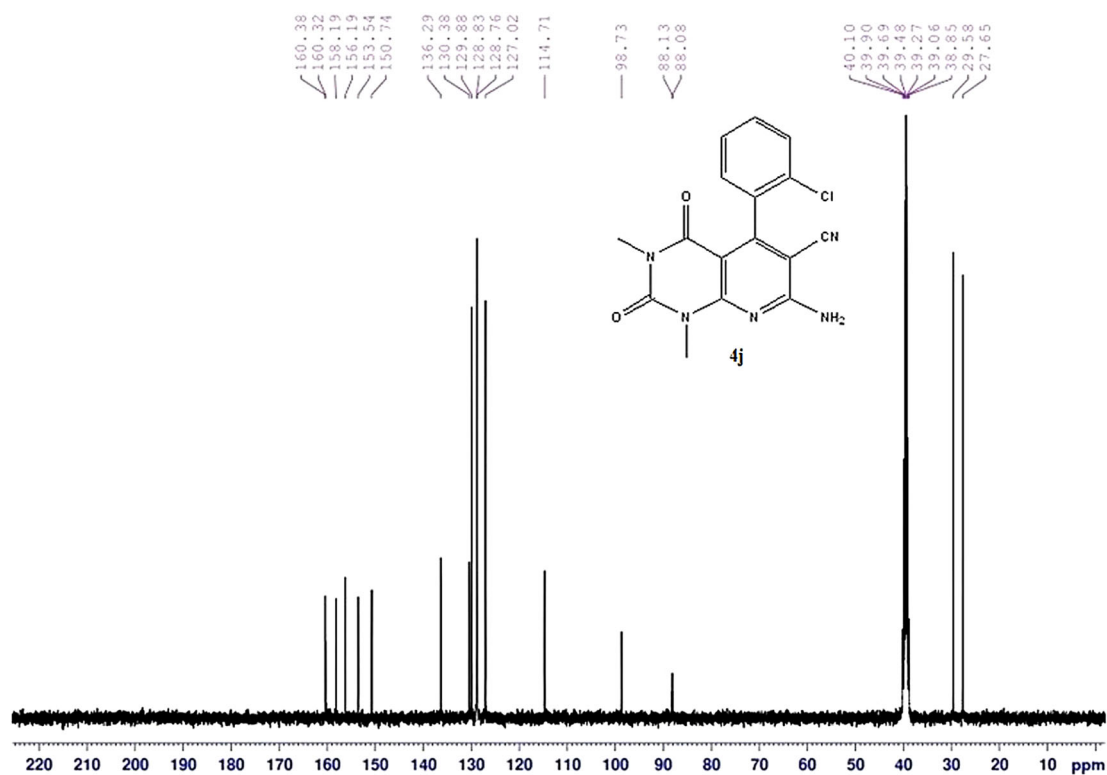


Fig. 10 ¹³C NMR spectra of 7-amino-5-(2-chlorophenyl)-1,3-dimethyl-2,4-dioxo-1,2,3,4-tetrahydropyrido[2,3-d] pyrimidine-6-carbonitrile

Fig. 11 ^1H NMR spectra of 7-amino-5-(3-bromophenyl)-1,3-dimethyl-2,4-dioxo-1,2,3,4-tetrahydropyrido[2,3-d]pyrimidine-6-carbonitrile

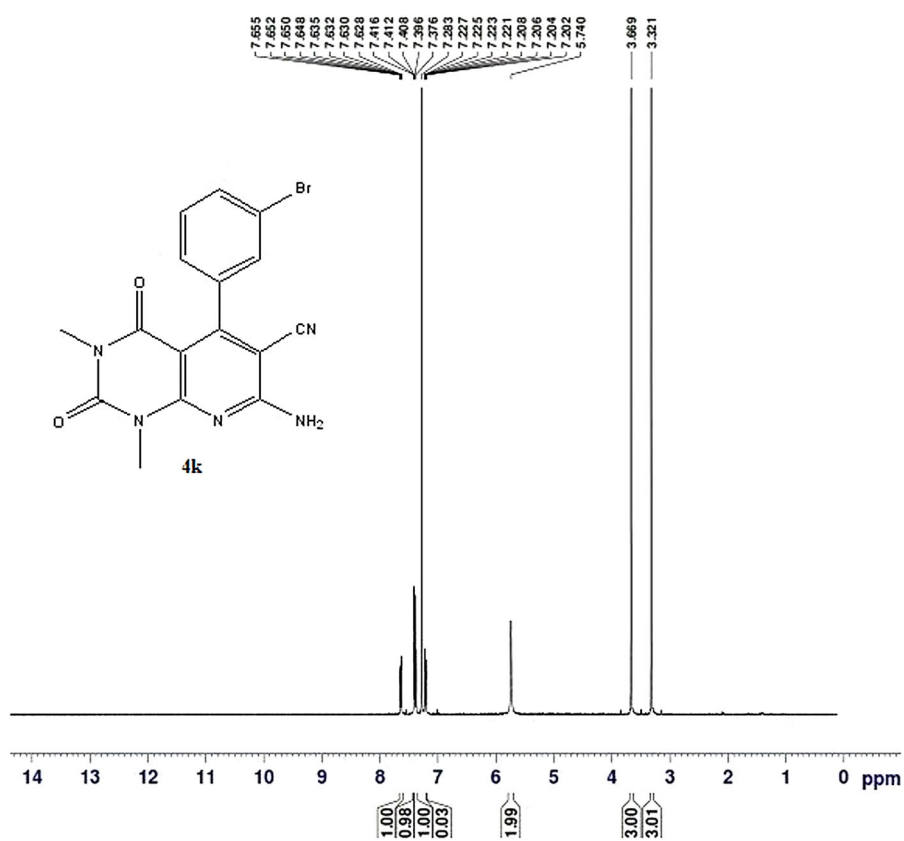
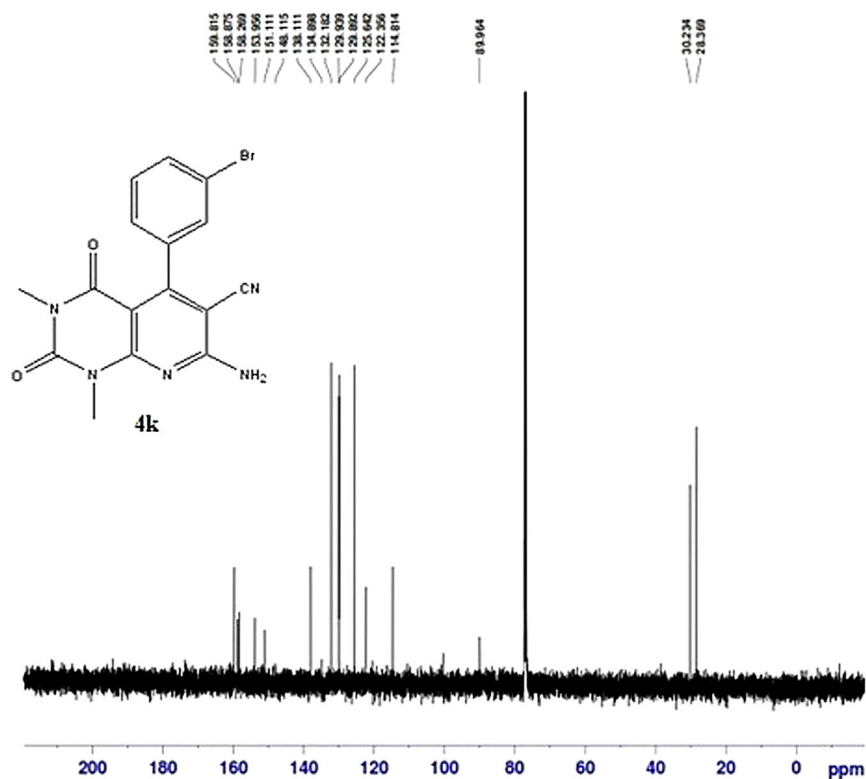


Fig. 12 ^{13}C NMR spectra of 7-amino-5-(3-bromophenyl)-1,3-dimethyl-2,4-dioxo-1,2,3,4-tetrahydropyrido[2,3-d]pyrimidine-6-carbonitrile



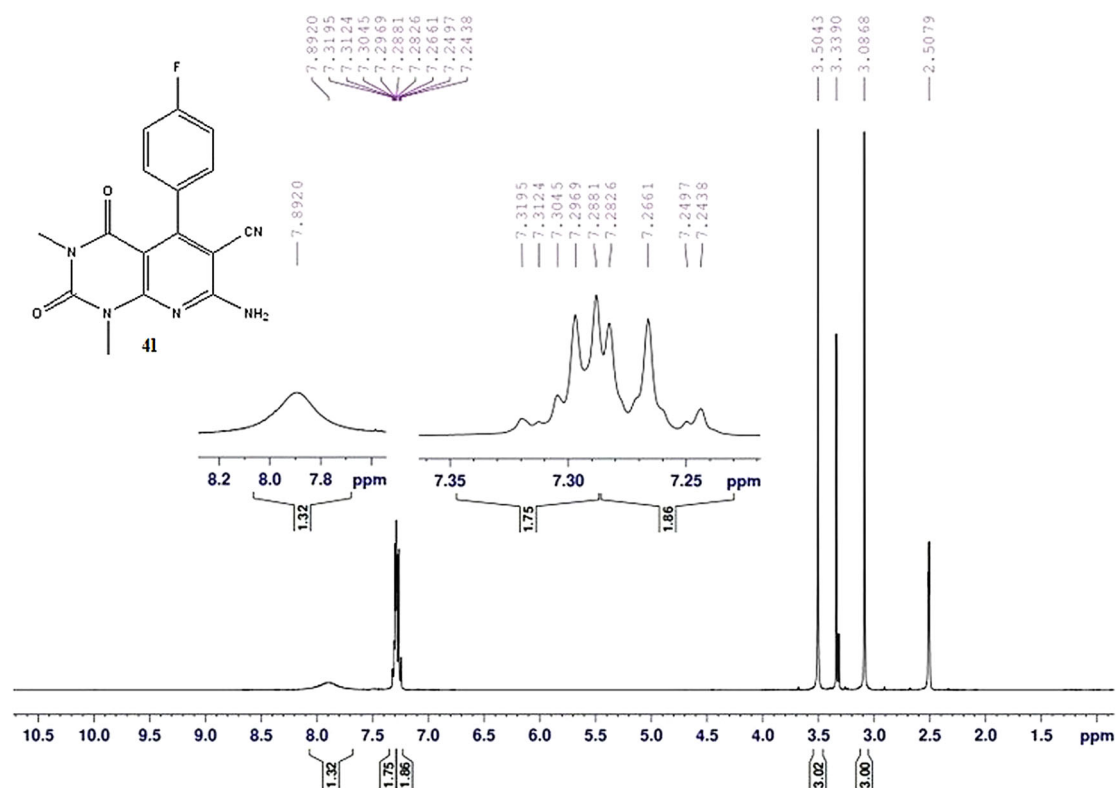


Fig. 13 ¹H NMR spectra of 7-amino-5-(4-fluorophenyl)-1,3-dimethyl-2,4-dioxo-1,2,3,4-tetrahydropyrido[2,3-d] pyrimidine-6-carbonitrile

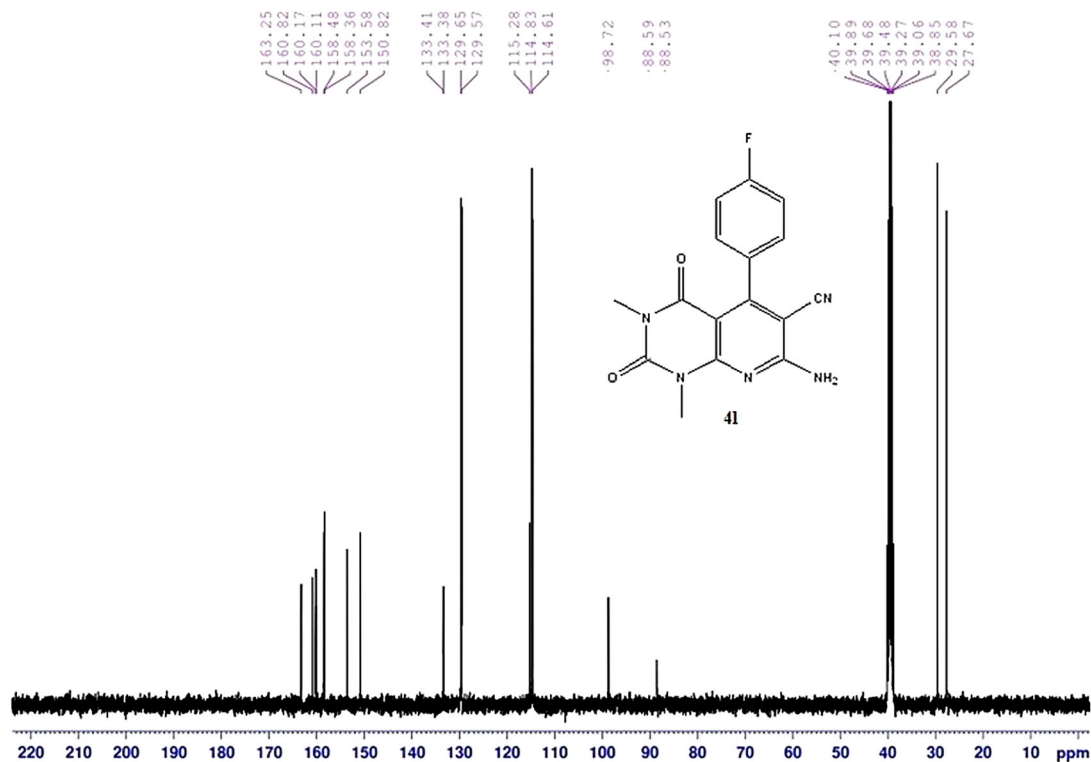


Fig. 14 ¹³C NMR spectra of 7-amino-5-(4-fluorophenyl)-1,3-dimethyl-2,4-dioxo-1,2,3,4-tetrahydropyrido[2,3-d] pyrimidine-6-carbonitrile

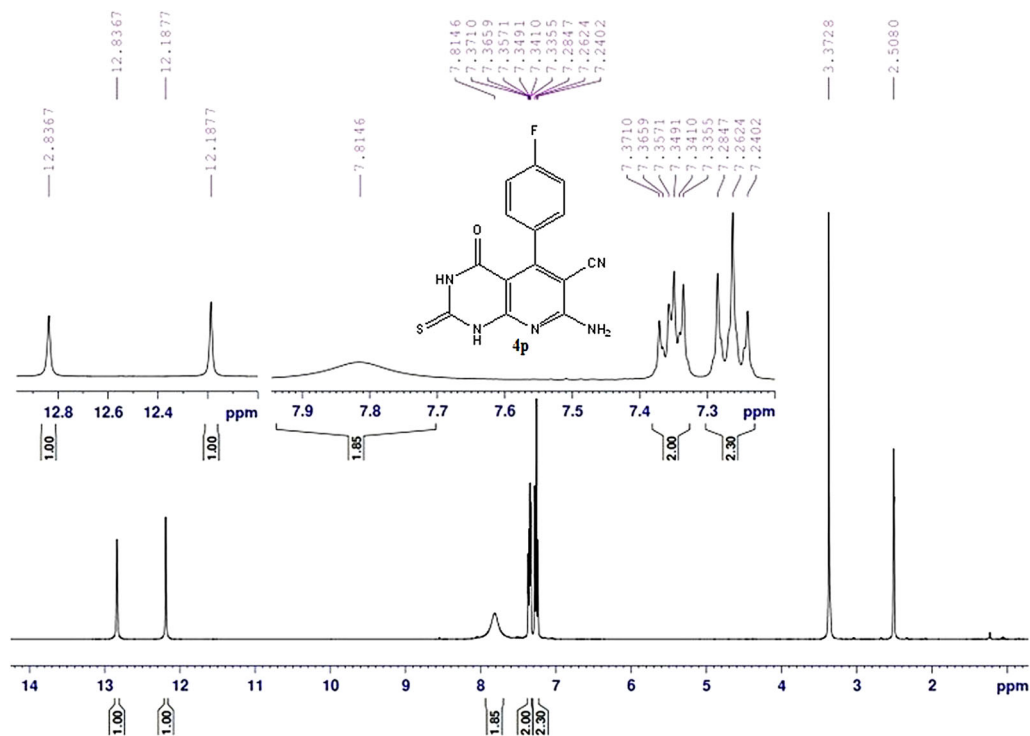


Fig. 15 ^1H NMR spectra of 7-amino-5-(4-fluorophenyl)-4-oxo-2-thioxo-1,2,3,4-tetrahydropyrido[2,3-d]pyrimidine-6-carbonitrile

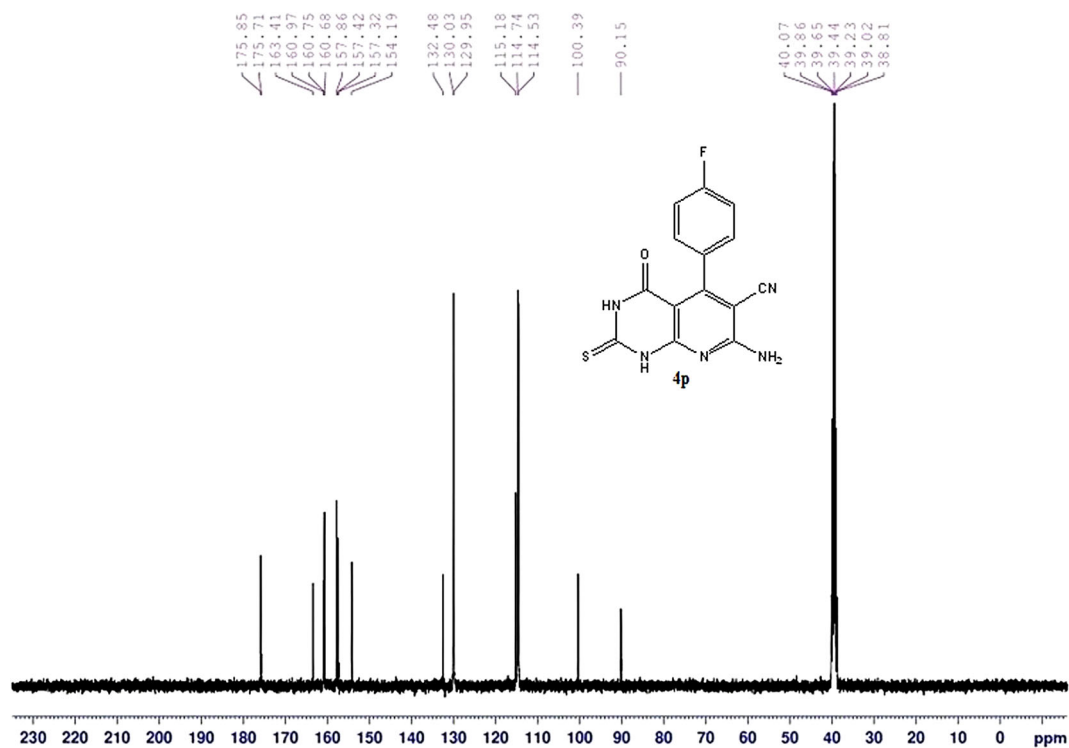


Fig. 16 ^{13}C NMR spectra of 7-amino-5-(4-fluorophenyl)-4-oxo-2-thioxo-1,2,3,4-tetrahydropyrido[2,3-d]pyrimidine-6-carbonitrile

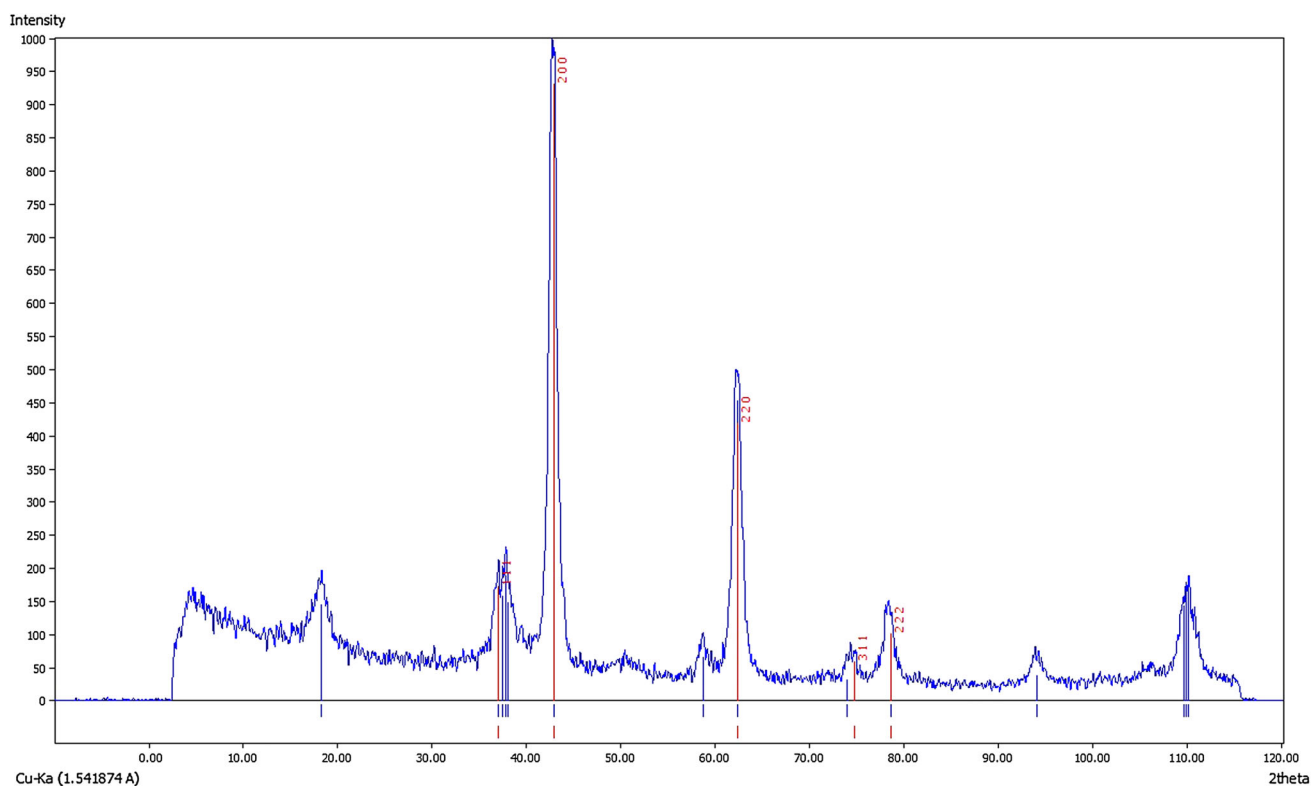


Fig. 17 X-ray powder diffraction pattern of nanocrystalline MgO

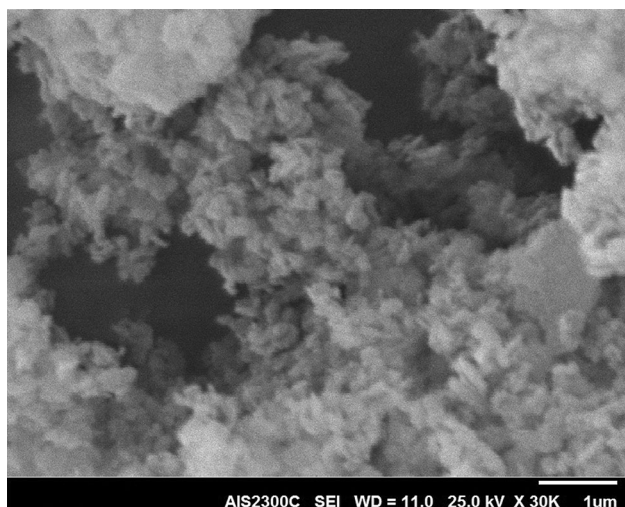


Fig. 18 SEM micrograph of nanocrystalline MgO

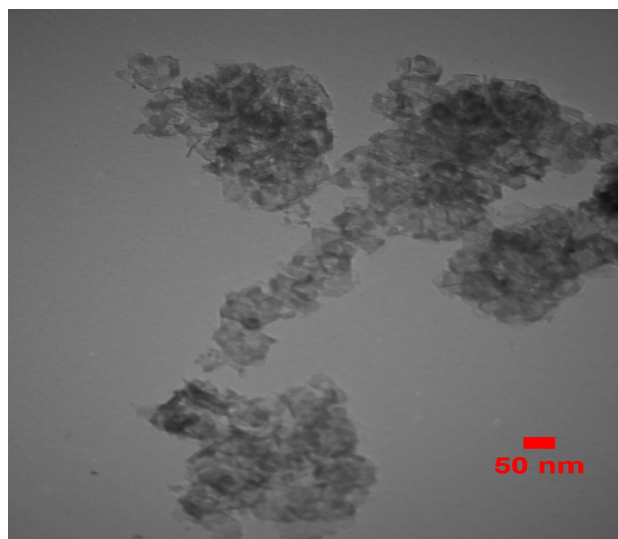


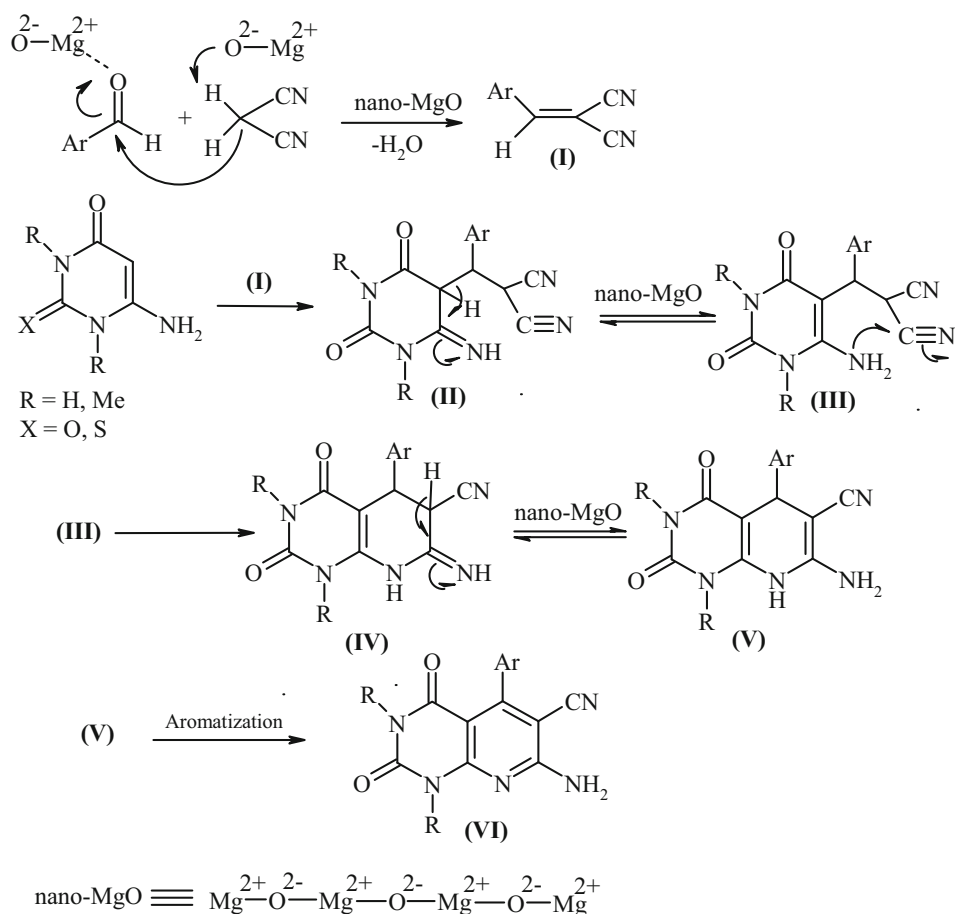
Fig. 19 TEM micrograph of nanocrystalline MgO

7-Amino-5-(4-fluorophenyl)-4-oxo-2-thioxo-1,2,3,4-tetrahydropyrido[2,3-d]pyrimidine-6-carbonitrile (4p)

Mp >300 °C. FT-IR (KBr): 3402, 3315, 3220 (NH stretch), 3087 (aromatic C–H stretch), 2214 (C≡N stretch), 1695, 1623 (C=O stretch), 1585, 1546

(aromatic C=C stretch), 1192 (C=S stretch), 1076 (C–F stretch), 802, 723 (aromatic C–H out of plane bending) cm^{-1} ; ^1H NMR (400 MHz, DMSO- d_6): δ : 7.26 (m, 2H), 7.35 (m, 2H), 7.81 (s, 2H, NH_2), 12.19 (s, 1H, NH), 12.84 (s, 1H, NH) ppm (Fig. 15); ^{13}C NMR (100 MHz, DMSO- d_6): δ : 175.8 (C=S), 175.7 (C=O



Scheme 2 A plausible mechanism for the pyrido[2,3-*d*]pyrimidines synthesis

amide), 163.4, 161.0, 160.7, 160.6, 157.8, 157.4, 157.3, 154.2, 132.5, 130.0, 115.2 (C≡N), 114.7, 100.4, 90.1 ppm (Fig. 16).

Results and discussion

The powder X-ray diffraction pattern of nanocrystalline MgO is shown in Fig. 17. All the diffraction peaks matched well with the face centered cubic structure of periclase MgO (JCPDS No. 87-0653). The major peaks at 2θ values of 37.1° , 43.0° , 62.4° , 74.8° and 78.6° can be indexed to the lattice planes of (111), (200), (220), (311) and (222) respectively.

The surface and textural morphology of the product was studied by SEM analysis. A closer view reveals that most of the nanocrystals have uniform diameter (Fig. 18).

The particle size was also examined using TEM. Figure 19 displays TEM micrographs of nanocrystalline MgO, revealing that the particle size is approximately 50 nm.

From BET analysis, the specific surface area of nanocrystalline MgO sample was found to be $63.32 \text{ m}^2/\text{g}$. A variety of pyrido[2,3-*d*]pyrimidines was prepared from arylaldehydes, 6-aminouracil, 6-amino-2-thiouracil or

Table 2 Recycling of nanocrystalline MgO for the preparation of **4a**

Run	1	2	3	4	5
Yield (%) ^a	92	90	88	87	86

^a All yields refer to isolated products

6-amino-1,3-dimethyluracil and malononitrile in the presence of nano-MgO in water at 80°C in excellent yields (Table 1, entries 1–16). It is worth mentioning that the corresponding pyrido[2,3-*d*]pyrimidines was isolated by crystallization from the crude filtrate. The results have been shown in Table 1. The reactions worked well with electron-donating and electron-withdrawing aldehydes. This three-component reaction proceeds via dual activation of substrates by nanocrystalline MgO which have a number of anionic oxidic Lewis basic O^{2-} and Mg^{2+} as Lewis acid site [21]. The Lewis base moiety of the catalyst activates the methylene group of malononitrile. The carbonyl oxygen of aldehyde coordinates with the Lewis acid moiety increasing the electrophilicity of the carbonyl carbon and thereby making it possible to carry out the reaction in short time. In a plausible mechanism, it is assumed that the reaction may proceed initially through the Knoevenagel condensation

between arylaldehyde and malononitrile to form intermediate **I**. Next, Michael addition of 6-aminouracils to intermediate **I** affords **II**. Intermediate **II** converts to **III** after tautomerization (nanocrystalline MgO can also act as a mild base for the deprotonation of an acidic proton of Intermediate **II**). Then, Intermediate **III** converts to **IV** via cyclization. Next, intermediate **IV** converts to **V** after tautomerization. Finally, the desired product **VI** is obtained after aromatization from **V** (Scheme 2).

It is notable that the bulk MgO shows lower catalytic activity than nanocrystalline MgO in this reaction and the products were obtained with lower yields and longer time. The high efficiency of the nanoparticle oxides is caused not only by their high surface area but also by the high concentration of low-coordinated sites and structural defects on their surface [22].

It is noteworthy to highlight that the nanocrystalline MgO could be recovered and reused without a significant loss of activity as illustrated in Table 2. After completion of the reaction, the product was extracted with ethyl acetate from the reaction mixture, and nanocrystalline MgO catalyst was separated out by centrifugation and the recovered catalyst was washed with ethanol followed by drying in an oven at 100 °C and reused as such for the subsequent reactions with fresh batch of reactants up to 5th run with only a slight loss its activity.

Conclusions

We have developed a simple, clean, efficient and one-pot procedure for the synthesis of pyrido[2,3-*d*]pyrimidines by the three-component condensation of aromatic aldehyde, 6-aminouracil, 6-amino-2-thiouracil or 6-amino-1,3-dimethyluracil and malononitrile using nanocrystalline MgO at 80 °C in water as a green solvent. Simple performance and work-up procedure and high yields are some of advantages of this method. Also, nanocrystalline MgO is recyclable and could be reused without significant loss of activity.

Acknowledgments We are grateful to Islamic Azad University of Rasht Branch for financial support.

Open Access This article is distributed under the terms of the Creative Commons Attribution 4.0 International License (<http://creativecommons.org/licenses/by/4.0/>), which permits unrestricted use, distribution, and reproduction in any medium, provided you give appropriate credit to the original author(s) and the source, provide a link to the Creative Commons license, and indicate if changes were made.

References

- Montreo, J.M., Brown, R., Gai, P.L., Lee, A.F., Wilsone, K.: In situ studies structure-reactivity relations in synthesis of bio-diesel over nanocrystalline MgO. *Chem. Eng. J.* **161**, 332 (2010)
- Narayanan, R., Ei-Sayed, M.A.: Shape dependent catalytic activity of platinum nanoparticles in colloidal solution. *Nano Lett.* **4**, 1343 (2004)
- Shi, F., Tse, M.K., Polhi, M.M., Bruckner, A., Zhang, S., Beller, M.: Tuning catalytic activity between homogenous and heterogeneous catalysis improved activity and selectivity of free nano-Fe₂O₃ in selective oxidations. *Angw. Chem. Int. Ed.* **46**, 8866 (2007)
- Grivaky, E.M., Lee, S., Siyal, C.W., Duch, D.S., Nichol, C.A.: Synthesis and antitumor activity of 2,4-diamino-6-(2,5-dimethoxybenzyl)-5-methylpyrido[2,3-*d*]pyrimidine. *J. Med. Chem.* **23**, 327 (1980)
- Furuya, S., Ohtaki, T.: Pyridopyrimidine derivatives, their production and use, Eur. Pat. Appl. EP. 608565 (1994)
- Heber, D., Heers, C., Ravens, U.: Positive inotropic activity of 5-amino-6-cyano-1,3-dimethyl-1, 2, 3, 4-tetrahydropyrido [2, 3-*d*] pyrimidine-2, 4-dione in cardiac muscle from guinea-pig and man. Part 6: compounds with positive inotropic activity. *Pharmazie* **48**, 537 (1993)
- DeGraw, J.I., Christie, P.H., Clowell, W.T., Sirotnak, F.M.: Synthesis and antifolate properties of 5,10-ethano-5,10-dideaza-aminopterin. *J. Med. Chem.* **35**, 320 (1992)
- Bradshaw, T.K., Hutchinson, D.W.: 5-Substituted pyrimidine nucleosides and nucleotides. *Chem. Soc. Rev.* **6**, 43 (1977)
- Quiroga, J., Cruz, S., Insuasti, B., Abonia, R.: Synthesis and structural analysis of 5-cyanodihydropyrazolo[3,4-*b*]pyrimidines. *J. Het. Chem.* **38**, 53 (2001)
- Thakur, A.J., Saikia, P., Prajapati, D., Sandhu, J.S.: Studies on 6-[(dimethylamino) methylene]aminouracils: a facile one-pot synthesis of pyrimido[4,5-*d*]pyrimidines and pyrido[2,3-*d*]pyrimidines, *Synlett*, 1299 (2001)
- Perez-Perez, M.J., Pretago, E.M., Jimeno, M.L., Camarasa M.J.: A new and efficient one-pot synthesis of pyrido[2,1-*f*]purine-2,4-diones starting from 6-aminouracil derivatives, *Synlett* 155 (2002)
- Bhuyan, P., Boruah, R.C., Sandhu, J.S.: Studies on uracils. 10. A facile one-pot synthesis of pyrido[2,3-*d*] and pyrazolo[3,4-*d*]pyrimidines. *J. Org. Chem.* **55**, 568 (1990)
- Muller, C.E., Geis, U., Hipp, J., Schobert, U., Frobenius, W., Pawlowski, M., Suzuki, F., Sandoval-Ramirez, J.: Synthesis and structure-activity relationships of 3,7-dimethyl-1-propargylxanthine derivatives, A2A-selective adenosine receptor antagonists. *J. Med. Chem.* **40**, 4396 (1997)
- Hirota, K., Kuki, H., Maki, Y.: Novel synthesis of pyrido[3,4-*d*]pyrimidines, pyrido[2,3-*d*]pyrimidines, and quinazolines via palladium-catalyzed oxidative coupling. *Heterocycles* **37**, 563 (1994)
- Srivastava, P., Saxena, A.S., Ram, V.J.: An elegant approach towards the regioselective synthesis of deazalumazines through nucleophile induced ring transformation reactions of 6-aryl-3-cyano-4-methylthio-2*H*-pyran-2-ones, *Synthesis* 541 (2000)
- Wang, X.S., Zeng, Z.S., Shi, D.Q., Wei, X.Y., Zong, Z.M.: KF-alumina catalyzed one-pot synthesis of pyrido[2,3-*d*]pyrimidine derivatives. *Synth. Commun.* **34**, 4331 (2004)
- Samai, S., Chandra Nandi, G., Chowdhury, S., Shankar Singh, M.: L-Proline catalyzed synthesis of densely functionalized pyrido[2,3-*d*]pyrimidines via three-component one-pot domino Knoevenagel aza-Diels–Alder reaction. *Tetrahedron* **67**, 5935 (2011)
- Yang, T., He, H., Ang, W., Yang, Y.H., Yang, J.Z., Lin, Y.N., Yang, H.C., Pi, W.Y., Li, Z.C., Zhao, Y.L., Luo, Y.F., Wei, Y.: Syntheses and cell-based phenotypic screen of novel 7-amino pyrido[2,3-*d*]pyrimidine-6-carbonitrile derivatives as potential antiproliferative agents. *Molecules* **17**, 2351 (2012)
- Abdolmohammadi, S., Balalaie, S.: An efficient synthesis of pyrido[2,3-*d*]pyrimidine derivatives via one-pot three-component reaction in aqueous media. *Int. J. Org. Chem.* **2**, 7 (2012)

20. Hussein, E.M.: Enviro-economic, ultrasound-assisted one-pot, three-component synthesis of pyrido[2,3-*d*]pyrimidines in aqueous medium. *Z. Naturforsch.* **67b**, 231 (2012)
21. Karmakar, B., Banerji, J.: A competent pot and atom-efficient synthesis of Betti bases over nanocrystalline MgO involving a modified Mannich type reaction. *Tetrahedron Lett.* **52**, 4957 (2011)
22. Safari, J., Zarnegar, Z., Heydarian, M.: Practical, ecofriendly, and highly efficient synthesis of 2-amino-4*H*-chromenes using nanocrystalline MgO as a reusable heterogeneous catalyst in aqueous media. *J. Taibah Uni. Sci.* **7**, 17 (2013)

